Biol Reprod. Author manuscript; available in PMC 2013 July 02.

Published in final edited form as:
Biol Reprod. 2013 June ; 88(6): 151. doi:10.1095/biolreprod.112.105759.

Analysis of Maternal and Fetal Cardiovascular Systems During Hyperglycemic Pregnancy in the Non-Obese Diabetic Mouse

Kristiina L. Aasa[1], **Kenneth K. Kwong**[1], **Michael A. Adams**[1], and **B. Anne Croy**[1]

[1]Department of Biomedical and Molecular Sciences, Queen's University, Kingston, ON Canada

Abstract

Pre-conception or gestationally-induced diabetes increases morbidities and elevates long-term cardiovascular disease risks in women and their children. Spontaneously hyperglycemic (d)-NOD/ShiLtJ females, a type 1 diabetes model, develop bradycardia and hypotension after midpregnancy compared with normoglycemic, age and gestation day (gd)-matched controls (c-NOD). We hypothesized that onset of the placental circulation at gd9–10 and rapid fetal growth from gd14 correlate with aberrant hemodynamic outcomes in d-NOD females. To develop further gestational time course correlations between maternal cardiac and renal parameters, high-frequency ultrasonography was applied to virgin and gd8–16 d- and c-NODs. Cardiac output and left ventricular (LV) mass increased in c- but not d-NODs. Ultrasound and postmortem histopathology showed overall greater LV dilation in d- than c-NOD mice in mid-late gestation. These changes suggest blunted remodeling and altered functional adaptation of d-NOD hearts. Umbilical cord ultrasounds revealed lower fetal heart rates from gd12 and lower umbilical flow velocities at gd14 and 16 in d- versus c-NOD pregnancies. From gd14–16, d-NOD fetal losses exceeded those of c-NOD. Similar aberrant responses in human diabetic pregnancies may elevate postpartum maternal and child cardiovascular risk, particularly if mothers lack adequate prenatal care or have poor glycemic control over gestation.

Keywords

Pregnancy; diabetes; NOD mouse; cardiovascular system; cardiac adaptations

INTRODUCTION

Pre-conception and gestational diabetes are common human pregnancy complications, occurring in 2–9% of pregnancies [1]. Both forms of diabetes increase maternal and fetal/neonatal morbidities [2, 3]. Since cardiovascular (CV) disease is strongly associated with diabetes [4], and pregnancy places enormous circulatory demands on women, it is not surprising that circulatory issues occur during and following diabetic pregnancies. Normal pregnancy is regarded as a CV "stress test" [5], in which reversible increases in blood

Corresponding Author: Dr. B Anne Croy, Queen's University, Department of Biomedical and Molecular Sciences, Botterell Hall 18 Stuart St. Kingston ON Canada, K7L3N6. Phone: 1 (613) 533-2859, Fax: 1 (613) 533-2566, croya@queensu.ca.

Funding support provided by Canadian Institutes for Health Research.

Presented in part at the 2012 Canadian Cardiovascular Congress, 27–31 October 2012, Toronto, Ontario.

volume (30–40%) [6], heart rate (20–30%) [7], cardiac output (CO) (30–60%) and cardiac hypertrophy (5–10% increase in mass) [6, 8] occur. Normally, these adaptive changes do not lead to increased blood pressure; instead, mean arterial pressure (MAP) declines or remains stable over gestation. This seemingly paradoxical outcome is attributed to systemic vasodilatation and vascular remodeling [9]. In diabetic women, circulatory adaptations to pregnancy may be incomplete or not fully reversed postpartum, causing persistent or subsequent changes that increase risk for CV diseases. Known elevated postpartum risks are reported for heart failure, coronary heart disease and stroke [10–14]. Since diabetes itself exacerbates CV disease progression, [13, 14] it is surprising that limited information is available concerning the functional and structural cardiac changes that occur in the pregnant diabetic female.

In contrast, the impact of maternal glycemic control on fetal and offspring health is well studied. For example, even with good glycemic control, increased incidences of macrosomia [15], intrauterine growth restriction (IUGR) [15] congenital heart defects, myocardial hypertrophy [15, 16] and death are reported in fetuses of diabetic women [15, 16]. Outcomes are more severe when glycemic control is suboptimal. Echocardiography is an effective clinical tool for assessing fetal well-being, developmental anomalies or distress [17, 18]. Postnatally, growth and development of offspring from diabetic gestations are accompanied by more CV events, obesity, diabetes, hypertension and metabolic syndrome [2, 11, 19].

The spontaneously diabetic NOD/ShiLtJ (d-NOD) mouse is widely used to model pathogenesis of CV disease in type 1 diabetes [3, 20–22]. Female NOD mice undergo spontaneous, selective destruction of the pancreatic islet cells from 12–30 weeks of age (later in males). Gradually, 90–100% of females turn hyperglycemic by 30 weeks of age. Prior to pancreatic islet cell destruction, animals are normoglycemic. This enables studies using normoglycemic litter-mates as age-matched controls when glycemic index is closely monitored. Pregnant, d-NOD females were studied by continuously monitored radiotelemetry in a non-anaesthetized state, which showed normal hemodynamic parameters until midpregnancy. The mice then became proteinuric and hypotensive in comparison to gestation day (gd)-matched normoglycemic (c)-NOD females, and had steadily declining mean arterial pressure (MAP) until parturition [20]. In addition to this unusual CV adaptation, fetal pathologies, resembling those in human diabetic gestations were reported [20]. Fetal neural tube and congenital cardiac defects are reported as the most frequent pathologies in human pregnancies complicated by pre-gestational diabetes [23]. Similarly, these defects are observed at high frequency in diabetic mouse pregnancies [20]. The timing of the discordance in MAP between d- and c-NODs [20] coincides with developmental opening of the mouse utero-placental circulation (gd 9–10 [24]). The hypothesis of the present study is that functional and structural cardiac responses to the physiological demands of mid-late pregnancy do not progress normally in d-NOD females. Demands such as the acute circulatory expansion resulting from onset of the utero-placental circulation and subsequent circulatory demands resulting from rapid, mid to late gestational fetal growth occur within this time-frame and provide the rationale for studying mid to late gestation. To address this hypothesis, high-frequency ultrasonography was employed to monitor maternal cardiac and renal function and structure before conception and between gd8–16 in d-NOD and c-NOD mice. Postmortem assessments of maternal hearts and kidneys were also

conducted. Fetal assessments were made by ultrasound examination of umbilical cord parameters between gd10–16. Progressive, atypical adaptation of maternal and fetal circulations was documented in d-NOD pregnancies over mid to late gestation.

MATERIALS AND METHODS

Animal Use

NOD/ShiLtJ (NOD) mice, 6–8 wk old, were obtained from The Jackson Laboratory (Bar Harbor, ME, USA). Blood glucose was quantified weekly in tail vein samples using OneTouch Ultra2 monitors and test strips (LifeScan, Burnaby, ON, Canada). Glucose values ≤9.9mmol/l were considered normoglycemic, 10.0–14.9mmol/l pre-diabetic and ≥15.0mmol/l, hyperglycemic. When a reading of ≥15.0mmol/l was obtained, daily blood glucose monitoring was employed to confirm the finding. Three consecutive days of hyperglycemic readings were used to define a mouse as diabetic. Once diabetic, females were immediately age-matched to a c-NOD female and both were paired with normoglycemic NOD males for breeding. Mean age of d-NOD females studied was 18.1±0.7 weeks with a range of 13–24 weeks; mean age of c-NOD females studied was 17.4±0.7 weeks with a range of 12–21 weeks. Detection of a copulation plug was considered gd0. Diabetic females received supplementary care, including moist chow, daily health checks and twice weekly body weight measurement to ensure stability. Glucose levels were measured prior to euthanasia to ensure a diabetic state had been maintained throughout pregnancy. Subcutaneous fluid (Lactated Ringer's Solution, 1ml) was administered daily at signs of dehydration. Animal usage was conducted in accordance with the SSR's specific guidelines and standards and under protocols approved by the Queen's University Animal Care Committee and in accordance with the Canadian Council on Animal Care's Guide to the Care and Use of Experimental Animals.

Ultrasonography

Females were imaged by ultrasound before mating or at gd8, 10, 12, 14 or 16, using a Vevo770 high-frequency, microultrasound system (VisualSonics, Toronto, ON, Canada). Three d-NOD and three c-NOD pregnancies were used per gd (total 30 pregnant and 6 virgin females scanned). Females were anesthetized with inhaled isofluorane (Pharmaceutical Partners of Canada Inc., Richmond Hill, ON, Canada), placed on the handling platform and had their limbs fixed to electrode plates using adhesive tape (Transpore; 3M, Maplewood, MN, USA), to enable monitoring of cardiac activity and respiration. Anaesthetic induction used 5% isoflurane in oxygen until the animals were inactive and moved to the handling platform. Anaesthesia was then was maintained between 1.5–2% isoflurane in oxygen. Heart rate was used as indicator of depth of anesthesia and used to ensure the lightest effective anesthetic depth was maintained. Depilatory cream (Nair; Church & Dwight Co. Inc, Princeton, NJ, USA) was used to remove fur over the ventral thorax, abdomen, and pelvis. Warmed, ultrasound-conducting gel (Ecogel 100; ECO-MED Pharmaceutical, Mississauga, ON, Canada) was placed between the area of interest and the ultrasound scanning head. Cardiac scans were conducted on the adult females using a 707B, 30MHz transducer to collect a left ventricular (LV) short axis M-mode cine loop at a mid-papillary level. Cardiac measurements were taken from this cine loop post-acquisition. Analyses included: LV trace,

LV inner and outer diameter, LV anterior and posterior wall thickness and LV chamber size. Vevo770 software used these measures to calculate CO, stroke volume (SV), ejection fraction (EF), fractional shortening (FS), LV diameter diastole and systole, LV volume diastole and systole, and LV mass. After completion of the cardiac scan, left and right renal scans were performed using the VisualSonics 704, 40MHz transducer. B-mode was used to visualize each kidney and its respective renal artery (RA) and vein (RV). Pulsed-wave (PW) Doppler signal was obtained for left and right RA. Post-acquisition measures were performed on peak systolic and end diastolic blood flow velocities. These values were used to determine renal Resistance Index (RI), calculated as [peak systolic flow velocity-end diastolic flow velocity/peak systolic flow velocity]. Then, for each pregnant female, a minimum of three fetuses were located and PW Doppler signals from the fetal umbilical arteries (UA) were recorded, with angle of insonation ≤ 60 degrees (angle correction was not performed). Non-viable fetuses were observed during some scans but were not used for recordings or analyses. Post-acquisition measurements for UA calculations included peak systolic blood flow velocities and fetal heart rate.

Histological Analyses

Upon completion of the ultrasound examination, mice were euthanized by an overdose of sodium pentobarbital (CEVA Sante Animale, Libourne, France) (50mg/kg) and exsanguinated via cardiac puncture. Hearts and kidneys were dissected and immersion fixed in 4% neutral-buffered paraformaldahyde (PFA; Sigma-Aldrich, Oakville, ON, Canada) followed by immersion in 70% ethanol. Tissues were then paraffin-embedded by standard automated processing. Sections from the 36 mice were cut onto slides at 3μm (kidney) or 6μm (heart) and two non-consecutive slides per animal were stained using i) Hematoxylin and Eosin (H&E) for general histology (heart and kidney), ii) periodic acid Schiff's reagent for glyoproteins (kidney), iii) Mason's trichrome for collagen deposition (heart) and iv) von Kossa's stain for mineral deposition (heart) using published protocols [25, 26]. Heart sections were digitized; ventricular wall width, interventricular septum length, ventricular lumen, and entire left ventricle areas from each heart were traced manually using Zeiss AxioVision Software (Carl Zeiss Canada Ltd., Toronto, ON, Canada). Morphometric analyses of kidneys included eight sequential cortical glomeruli that were assessed under high power, oil immersion microscopy from each PAS-stained kidney section. Glomeruli were scored semi-quantitatively as described by others [27], between 0–4 depending on severity of pathology present (0=normal; 4=very severe capillary loop occlusion with hypercellularity).

Statistical Analyses

Ultrasound data were analyzed using Prism Statistical Software (GraphPad, San Diego, CA, USA). Data are presented as mean ± standard error of the mean (SEM), and were calculated using n=3/group for all maternal data and n≥9/group for all fetal data (minimum 3 fetuses from each of 3 dams/group). Echocardiographic data were normalized to litter size (values were divided by the number of live pups) to account for differences of litter size within groups. Two-way ANOVA and linear regression were performed for statistical comparisons. Regressions with non-zero slopes were considered significant at $p \leq 0.05$ and used to define a change over time within a group. Differences in changes over time between groups were

defined by testing the difference between slopes. Differences were considered significant at $p \leq 0.05$ and non-statistically significant trends were defined at $p \leq 0.15$. Bonferroni's post-test was used to investigate differences between groups at specific gestation days.

RESULTS

General Features of NOD Pregnancies

Diabetic NODs were age-matched to c-NODs for breeding. As shown in Table 1, preconception body weights and gd-matched weights at times of ultrasound scans did not differ between groups. Number of viable pups differed between study pairs, but on average were similar between groups (mean = 8.67 fetuses for d-NOD (range of 1–11) and mean = 8.67 fetuses for c-NOD (range of 4–12)) (Table 1).

Cardiac assessments in d-NOD and c-NOD before conception and at gd8

Echocardiography of virgin and gd8 mice showed no differences between diabetic and control females in any parameter measured (CO, SV, LV diastolic diameter, LV mass or FS). Histopathology and morphometric measures at these time-points also showed no differences. This indicated that heart structure and function were the similar in all females prior to mating and in early pregnancy, prior to opening of the placental circulation.

Maternal cardiac adaptations from gd10–16

Ultrasound—Cardiac output (a function of SV and heart rate) was normalized to account for variations in litter sizes within groups and over time (Table 1). In rats, litter size is reported as positively correlated with CO and negatively correlated with MAP and vascular resistance [28]. Illustrated in FIG. 1A and 1B are representative parasternal short axis B-Mode and M-Mode views of the maternal heart upon which calculations were based. Papillary muscle was used to determine location within the chamber and maintain consistency across scans. Once normalized, CO was increased in c-NODs over the measured gestational time-points ($p=0.0246$; FIG. 1C). This was attributed primarily to increases in SV (FIG. 1D) since the heart rates were stabilized to the same range on each gd. In contrast to c-NODs, neither CO nor SV increased in d-NODs over gestation (FIG. 1C, 1D). Changes in CO and SV over gestation differed between groups as shown by the finding of significantly different slopes in regression analysis ($p=0.024$ and $p=0.030$, respectively).

Fractional shortening measures the proportion of LV diastolic diameter that is lost in systole and is a surrogate measure for LV systolic function [29]. In normal, non-pregnant humans the expected range in FS is from 27 to 45% [30]. Overall, FS was higher in d-NOD compared to c-NOD over the intervals measured (determined by two-way ANOVA), however no differences were observed at any particular gd (by Bonferroni post-test) and no effect of gestation was seen in either group (determined by linear regression) (FIG. 1E). When normalized to heart rate (by dividing FS by heart rate), the same outcome of increased FS in d-NOD compared to c-NODs was observed ($p=0.0037$, data not shown). Left ventricular diastolic diameter, measured by ultrasound, did not increase in d-NOD ($p=0.4158$) mice across mid to late gestation but increased in c-NOD mice (statistically non-zero slope, $p=0.0135$). The effect of gestation on LV diastolic diameter differed between d-

and c-NOD, demonstrated by a difference in slopes by linear regression (p=0.017) (FIG. 2A). Over the study interval, d-NOD hearts showed no measurable increase in LV mass, adjusted to litter size and calculated from ultrasound measurements. In contrast, LV mass of c-NODs increased over mid to late gestation (FIG. 2B), reflecting the LV hypertrophy expected in normal pregnancy.

Histopathology—Histopathology of d-NOD left ventricles showed no visible lesions at the gestational time-points studied (FIG 2C). Morphometric analyses revealed differences in LV dilation between the diabetic and control mice. The d-NOD hearts had a greater LV lumen to total LV area ratio than gd10–16 controls heart; analysis at specific gestation days revealed differences between groups at gd14 (FIG 2D). Virgin and gd8 hearts were also studied and no differences were found between groups at either time-point, indicating that changes occur after opening of the utero-placental circulation.

Renal Analyses

Kidneys play a major role in blood pressure regulation and undergo substantial alteration during normal pregnancy, including increases in size, volume, glomerular filtration rate and effective renal plasma flow rate [31]. Renal RI, as calculated by ultrasonography, is an indicator for downstream vascular impedance and correlates inversely with changes in renal blood flow expected during normal pregnancy [31]. Figures 3A and 3B illustrate B mode and PW-Doppler renal scans typical of those used for calculations. Renal artery RI did not differ between virgin d-NOD and c-NOD mice or at any gestation time-point studied (FIG 3C). No structural anomalies were observed in any kidneys via B-Mode imaging (FIG. 3A).

Glomerular changes are the earliest and most frequently observed renal histopathology. Blinded, semi-qualitative analysis was performed to assess mesangial matrix expansion and hypercellularity. No quantitative differences in glomerular histology were detected between d-NOD and c-NOD kidneys at any time-point studied (FIG 3D, FIG 3E).

Fetal Umbilical Cord Analyses

Umbilical flow rates were not detectable in NOD fetuses prior to gd10. From gd10 onwards, fetus, placenta and umbilical cord were easily visualized with B-Mode ultrasonography. Figure 4A shows a typical B-Mode image of the umbilical cord and placenta of a gd10 c-NOD fetus while Figure 4B shows a typical gd10 PW Doppler scan of the same fetus. Pulsatility of the umbilical artery is used to differentiate between umbilical artery and vein in PW Doppler, with the extent of pulsatility increasing from gd10 (FIG. 4B) to gd16 (FIG. 4C). Overall analyses between gd10–16 showed that fetuses of d-NOD dams had lower umbilical peak and mean flow velocities than fetuses of c-NOD dams ($p<0.0001$; FIG 4D, FIG 4E). Umbilical artery Resistance Index was also lower in fetuses of diabetic dams compared to controls (p=0.013, data not shown). Differences at specific gd reached significance at gd14 and 16 ($p<0.001$, $p<0.05$ respectively). In fetuses of c-NOD dams, umbilical artery peak flow velocities increased over mid to late gestation (p=0.0012). This was blunted in fetuses of d-NOD dams, with a non-statistically significant trend towards an increase in umbilical flow velocities over mid to late gestation (p=0.0558). Heart rates in fetuses of both c-NOD and d-NOD pregnancies increased between gd10 and 16 ($p<0.0001$,

p=0.0051 respectively) but patterns and extent of increases differed between the groups. Fetuses of d-NOD pregnancies had lower heart rates overall than fetuses of c-NOD pregnancies (p=0.0002). Differences between groups peaked at gd12 and 14 ($p<0.05$, $p<0.01$ respectively; FIG 4F). The onset of lower heart rates in fetuses of d-NOD females at gd12 and lower umbilical flow velocities at gd14 suggest that diabetic pregnancies become compromised subsequent to gd10. This was further exemplified by postmortem enumeration of failed implantation sites with increased fetal loss seen in later gestation days (gd14 and 16) in d-NOD compared to c-NODs (FIG. 4G).

DISCUSSION

Ultrasound study of d- and c-NOD mice revealed times of onset and progression of functional differences in adaptations of maternal and fetal CV systems that appear to be attributed to hyperglycemia. In pregnant females, diabetes promoted an excessively dilated left ventricle and blunted rise in cardiac output and stroke volume after gd12. Fetal impairments were clearly present from gd12 as lower heart rates and at gd14 as lower umbilical artery flow velocity. These findings suggest either fetal alterations are occurring before the atypical changes in maternal cardiovascular adaptation, or, there are maternal changes at gd10–12 that are not detectable by our study techniques. Completion of fetal and placental development (gd12) and initiation of rapid fetal growth (gd14) [32] are the developmental events coinciding with the timing of the atypical responses observed here.

Diabetes alone is known to increase risk for the development of heart failure due to a decrease in myocardial contractile function (diabetic cardiomyopathy). In diabetic mouse models, decreased systolic function has been noted at one year after onset of hyperglycemia [4]. Since the females in this study were mated at onset of diabetes, and their cardiac ultrasound profiles at mating did not differ from c-NOD females, cardiomyopathy was unlikely to have been present at conception. Maternal age differences in time-dependent progression of the diabetic state are present in this study, however, mean ages vary by less than 5%. Previous work by Burke *et al* 2011 (reported in their supplementary materials) showed that non-pregnant, d-NOD females were hemodynamically stable (measured by continuous radiotelemetry) over the first 13 days following hyperglycemic conversion. Differences in heart rate were only observed in pregnant animals of similar age after midgestation [20]. Another study on non-pregnant, female NOD mice (from a different supplier) reported onset of bradycardia at day 28, their first measurement after diabetic onset [33]. Thus the cardiac changes seen in the current study by day 16 after diabetic onset are more likely to be pregnancy-induced rather than solely diabetes-induced, although the latter cannot be completely discounted. Indeed, the pattern observed here of onset of functional cardiac anomaly after midgestation is consistent with previous work, in which the hemodynamic profiles (measured by radiotelemetry) of d- and c-NOD mice, were concordant until gd10. Subsequently MAP and heart rate began to diverge, with lower MAP and heart rate in d-NODs compared to controls [20]. Both studies, using very different technical approaches, identify midgestation as a critical period for development of cardiac pathologies during diabetic pregnancy.

Opening of the placental circulation was postulated to pose an acute demand on the maternal CV system that could not be met in hyperglycemic pregnancy. In the present study, CO, used as a measure of cardiac function, followed the expected pattern of gestational increase in c-NODs. This suggests that c-NOD hearts are better equipped to meet increased placental and fetal demands. Cardiac output in d-NODs did not increase over this interval, indicating a failure to adapt in a physiological manner. Stroke volume followed the same pattern, with very little difference in p values, and a reduction from gd10 to gd16 of approximately 29% (compared to a 37% reduction in CO). This indicates that the bradycardia observed in d-NODs is only minimally responsible for the resulting effects on CO and that SV is the major contributor. This effect on SV resembles the blunted increases in CO and LV diastolic diameter reported in diabetic pregnant women [34] and in CO and SV reported in a postpartum study of women with previous gestational diabetes [35]. In the latter study, the gestationally diabetic women at 1–4 years postpartum had markers of endothelial dysfunction (altered flow-mediated dilatation), and subclinical inflammation (elevated Interleukin 6, c-reactive protein), both predictive of increased future CV disease risk [35]. The increased FS in d-NOD compared to c-NOD is an interesting finding when combined with the observed bradycardia. This phenomenon is not documented in the literature and may be a type of compensation for the decreased heart rate and failure to acquire normal increases in CO. Increased FS may result from decreased heart rate in d-NOD mice. A slower heart rate would allow more time for ventricular filling, resulting in increased ventricular stretch, greater diastolic volume and increased LV contractile strength, according to the Frank-Starling law of the heart [36]. Postmortem findings reported here support the conclusion drawn from the maternal echocardiography, that the cardiac responses to pregnancy differed between d-NOD and c-NOD females. Development of transient cardiac hypertrophy is expected in normal pregnancy [6] and was observed in c-NOD as increasing LV mass over late gestation. This adaptation, which typically reverses postpartum [8], did not occur in d-NOD hearts. Additionally, d-NOD but not c-NOD hearts showed increasing lumen area to total ventricular area ratios, suggesting progressive dilation over mid to late gestation. The increased ratio results mainly from increased d-NOD lumen areas (data not shown). Differences in LV diastolic diameter (obtained by M-mode ultrasound), however, are not observed between d- and c-NOD. Methodological differences are believed to account for this apparent discrepancy since the maximally relaxed, intact heart was measured *in vivo* along a single plane in one-dimension using ultrasound, while fixed hearts, in which some shrinkage would be expected from fixation and processing, were assessed in cut sections by repeated measures in two dimensions.

Myocyte death is an expected step in the pathogenesis of dilated cardiomyopathy [37]. In streptozotocin-induced diabetes, myocyte apoptosis increased in male rat hearts with highest levels reported at day 3 after drug treatment and declining numbers of apoptotic cells to day 28 of study [38]. Of interest, myocyte apoptosis was inversely related to blood glucose levels that increased over the 3–28 day post-treatment interval suggesting that streptozotocin itself contributes to myocyte death. This confounds interpretation of the effects of hyperglycemia on myocyte viability in this model. Since blood glucose values in the treated rats and in gd10 d-NOD mice were similar, the apparent lack of histopathology in the mouse hearts in the current study suggests that the more gradual onset of diabetes in NOD mice may be a

less pathologic process for myocytes [39]. Further study will be required to define the potential role of cardiac apoptosis in the LV dilation observed in d-NODs over late gestation.

Circulatory control involves integrated responses between the cardiovascular and renal systems. Neither ultrasound study of the living kidney nor post-mortem histopathology revealed gestational differences between d-NOD and c-NOD kidneys. These findings reinforce our conclusion that the heart is a key player in the pathogenesis and development of anomalous CV responses during diabetic pregnancy. Blood vessels and hormones also play important roles in cardiac adaptations to pregnancy but were not addressed in our study [40]. Insulin from slow release implants was not used in this study and due to this lack of disease control, greater handling was required of the experimental animals compared with their controls. This included more frequent weighting, and subcutaneous fluids at a frequency of up to once per day. Handling stress may also have contributed in a minor way to the observed differences. The need for anaesthetic during ultrasound scanning, and individual variations in responses to inhaled anaesthetic are limitations of rodent ultrasonography and should be considered when interpreting results.

The impact of diabetes on fetal health was detected by umbilical artery velocimetry as lower d-NOD fetal heart rate and umbilical flow velocity compared to c-NOD. Both peak and mean umbilical artery flow velocities were assessed to assure that mean flow had not been elevated in d-NOD to compensate for their lower peak umbilical flow velocity. The increased incidence of fetal cardiac defects in diabetic pregnancy [2, 23] may contribute to the differences in fetal heart rates observed between d-NOD and c-NOD mice. Umbilical artery velocities are thought to reflect fetoplacental blood flow and to be correlated with total placental volume blood flow, which is decreased in cases of growth-restricted fetuses [41]. Clinically, umbilical artery velocimetry is also useful as a predictive measure of fetal outcome in small for gestation age infants [42]. Recently others reported no difference in fetal heart rates or fetal aortic flow velocity between normoglycemic and hyperglycemic dams (mated after induction of diabetes using streptozotocin) [43]. Thus the method by which hyperglycemia develops, and its speed of onset, may also influence the fetal environment and result in differing fetal cardiovascular phenotypes between animal models. The NOD mouse model shows vascular lesions, IUGR, neural tube and congenital heart defects similar to fetuses and offspring of human diabetics [13, 18, 20, 21, 23]. Previous study of term pregnancies in d-NOD indicated neonates were smaller than offspring of c-NOD females [20]. In the present study, increased fetal death was observed in gd14–16 d-NOD compared to c-NOD litters. Thus, ultrasound study of mouse fetuses has predictive values similar to clinical ultrasound, and the d-NOD mouse appears to be a strong animal model for advancing current knowledge on the effects of hyperglycemia on the maternal CV system during human pregnancy.

Prenatal care and glycemic control of pregnant diabetic women have been improving in urban regions of developed countries. However, in areas with limited health care access and in studies of unselected populations, increased fetal and maternal morbidities and mortality are still found in diabetic compared to normoglycemic pregnancies. Even in more advanced health care centers, increased prenatal care for diabetic women compared to routine care resulted in decreased perinatal morbidity and increased maternal quality of life [1]. A study

of patients from Britain found that only 7% of type 1 diabetic women had optimal glycemic control at their first antenatal visit (approximately 9th wk of gestation) [44]. A peak period of sensitivity to lack of glycemic control has been identified as 8–16 wk of human gestation [45]. These data align with the results reported here and suggest that opening of the uteroplacental circulation (gd9–10 in mice and approximately 12 weeks gestation in humans), followed by the onset of rapid fetal growth, are the physiological drivers promoting life-long CV consequences following a diabetic pregnancy. Results of this study help to stress the importance of optimal glycemic control in diabetic pregnancy as being key to the ever-increasing co-prevalence of diabetes and CV disease in postpartum diabetic women.

Acknowledgments

The authors thank Dr. Graeme Smith, Ms. Tiziana Cotechini and Ms. Wilma Hopman for invaluable advice and assistance with data analysis. We also thank Dr. Jianhong Zhang, Mr. Richard Di Lena, Ms. Jalna Meens, Mr. Alexander Hofmann and Mr. Andrew Kriger for technical support.

References

1. Crowther CA, Hiller JE, Moss JR, McPhee AJ, Jeffries WS, Robinson JS. Effect of treatment of gestational diabetes mellitus on pregnancy outcomes. N Engl J Med. 2005; 352:2477–2486. [PubMed: 15951574]
2. Hay WW Jr. Care of the Infant of the Diabetic Mother. Curr Diab Rep. 2011
3. Vambergue A, Fajardy I. Consequences of gestational and pregestational diabetes on placental function and birth weight. World J Diabetes. 2011; 2:196–203. [PubMed: 22087356]
4. Tarquini R, Lazzeri C, Pala L, Rotella CM, Gensini GF. The diabetic cardiomyopathy. Acta Diabetol. 2011; 48:173–181. [PubMed: 20198391]
5. Craici I, Wagner S, Garovic VD. Preeclampsia and future cardiovascular risk: formal risk factor or failed stress test? Ther Adv Cardiovasc Dis. 2008; 2:249–259. [PubMed: 19124425]
6. Hunter S, Robson SC. Adaptation of the maternal heart in pregnancy. Br Heart J. 1992; 68:540–543. [PubMed: 1467047]
7. Desai DK, Moodley J, Naidoo DP. Echocardiographic assessment of cardiovascular hemodynamics in normal pregnancy. Obstet Gynecol. 2004; 104:20–29. [PubMed: 15228996]
8. Tsiaras S, Poppas A. Cardiac disease in pregnancy: value of echocardiography. Curr Cardiol Rep. 2010; 12:250–256. [PubMed: 20424969]
9. Burke SD, Barrette VF, Carter AL, Gravel J, Adams MA, Croy BA. Cardiovascular adaptations of pregnancy in T and B cell-deficient mice. Biol Reprod. 2011; 85:605–614. [PubMed: 21613629]
10. Kitzmiller JL, Dang-Kilduff L, Taslimi MM. Gestational diabetes after delivery. Short-term management and long-term risks. Diabetes Care. 2007; 30 (Suppl 2):S225–235. [PubMed: 17596477]
11. Simeoni U, Barker DJ. Offspring of diabetic pregnancy: long-term outcomes. Semin Fetal Neonatal Med. 2009; 14:119–124. [PubMed: 19208505]
12. Dawson SI. Glucose tolerance in pregnancy and the long-term risk of cardiovascular disease. Diabetes Res Clin Pract. 2009; 85:14–19. [PubMed: 19446355]
13. Haeri S, Khoury J, Kovilam O, Miodovnik M. The association of intrauterine growth abnormalities in women with type 1 diabetes mellitus complicated by vasculopathy. Am J Obstet Gynecol. 2008; 199:278 e271–275. [PubMed: 18771982]
14. Burke SD, Dong H, Hazan AD, Croy BA. Aberrant endometrial features of pregnancy in diabetic NOD mice. Diabetes. 2007; 56:2919–2926. [PubMed: 17827401]
15. Evers IM, de Valk HW, Visser GH. Risk of complications of pregnancy in women with type 1 diabetes: nationwide prospective study in the Netherlands. BMJ. 2004; 328:915. [PubMed: 15066886]

16. Platt MJ, Stanisstreet M, Casson IF, Howard CV, Walkinshaw S, Pennycook S, McKendrick O. St Vincent's Declaration 10 years on: outcomes of diabetic pregnancies. Diabet Med. 2002; 19:216–220. [PubMed: 11918624]
17. Mongiovi M, Fesslova V, Fazio G, Barbaro G, Pipitone S. Diagnosis and prognosis of fetal cardiomyopathies: a review. Curr Pharm Des. 2010; 16:2929–2934. [PubMed: 20632954]
18. Turan S, Turan OM, Miller J, Harman C, Reece EA, Baschat AA. Decreased fetal cardiac performance in the first trimester correlates with hyperglycemia in pregestational maternal diabetes. Ultrasound Obstet Gynecol. 2011; 38:325–331. [PubMed: 21538641]
19. Bunt JC, Tataranni PA, Salbe AD. Intrauterine exposure to diabetes is a determinant of hemoglobin A(1)c and systolic blood pressure in pima Indian children. J Clin Endocrinol Metab. 2005; 90:3225–3229. [PubMed: 15797952]
20. Burke SD, Barrette VF, David S, Khankin EV, Adams MA, Croy BA. Circulatory and renal consequences of pregnancy in diabetic NOD mice. Placenta. 2011; 32:949–955. [PubMed: 22014504]
21. Bucci M, Roviezzo F, Brancaleone V, Lin MI, Di Lorenzo A, Cicala C, Pinto A, Sessa WC, Farneti S, Fiorucci S, Cirino G. Diabetic mouse angiopathy is linked to progressive sympathetic receptor deletion coupled to an enhanced caveolin-1 expression. Arterioscler Thromb Vasc Biol. 2004; 24:721–726. [PubMed: 14962949]
22. Zimmerman MA, Haskins K, Bradley B, Gilman J, Gamboni-Robertson F, Flores SC. Autoimmune-mediated vascular injury occurs prior to sustained hyperglycemia in a murine model of type I diabetes mellitus. J Surg Res. 2011; 168:e195–202. [PubMed: 21470634]
23. Corrigan N, Brazil DP, McAuliffe F. Fetal cardiac effects of maternal hyperglycemia during pregnancy. Birth Defects Res A Clin Mol Teratol. 2009; 85:523–530. [PubMed: 19180650]
24. Adamson SL, Lu Y, Whiteley KJ, Holmyard D, Hemberger M, Pfarrer C, Cross JC. Interactions between trophoblast cells and the maternal and fetal circulation in the mouse placenta. Dev Biol. 2002; 250:358–373. [PubMed: 12376109]
25. AFIP Laboratory Methods in Histotechnology. Washington, DC: American Registry of Pathology; 1992.
26. Moon JY, Tanimoto M, Gohda T, Hagiwara S, Yamazaki T, Ohara I, Murakoshi M, Aoki T, Ishikawa Y, Lee SH, Jeong KH, Lee TW, et al. Attenuating effect of angiotensin-(1–7) on angiotensin II-mediated NAD(P)H oxidase activation in type 2 diabetic nephropathy of KK-A(y)/Ta mice. Am J Physiol Renal Physiol. 2011; 300:F1271–1282. [PubMed: 21367916]
27. Wang H, Madhusudhan T, He T, Hummel B, Schmidt S, Vinnikov IA, Shahzad K, Kashif M, Muller-Krebs S, Schwenger V, Bierhaus A, Rudofsky G, et al. Low but sustained coagulation activation ameliorates glucose-induced podocyte apoptosis: protective effect of factor V Leiden in diabetic nephropathy. Blood. 2011; 117:5231–5242. [PubMed: 21389321]
28. Ahokas RA, Sibai BM. The relationship between experimentally determined litter size and maternal blood pressure in spontaneously hypertensive rats. Am J Obstet Gynecol. 1990; 162:841–847. [PubMed: 2316595]
29. Otto, CM., Pearlman, AS. Textbook of clinical echocardiography. Philadelphia: W.B. Saunders; 1995.
30. Locatelli P, Olea FD, De Lorenzi A, Salmo F, Vera Janavel GL, Hnatiuk AP, Guevara E, Crottogini AJ. Reference values for echocardiographic parameters and indexes of left ventricular function in healthy, young adult sheep used in translational research: comparison with standardized values in humans. Int J Clin Exp Med. 2011; 4:258–264. [PubMed: 22140597]
31. Ogueh O, Clough A, Hancock M, Johnson MR. A longitudinal study of the control of renal and uterine hemodynamic changes of pregnancy. Hypertens Pregnancy. 2011; 30:243–259. [PubMed: 21740248]
32. Mu J, Adamson SL. Developmental changes in hemodynamics of uterine artery, utero- and umbilicoplacental, and vitelline circulations in mouse throughout gestation. Am J Physiol Heart Circ Physiol. 2006; 291:H1421–1428. [PubMed: 16603699]
33. Gross V, Tank J, Partke HJ, Plehm R, Diedrich A, da Costa Goncalves AC, Luft FC, Jordan J. Cardiovascular autonomic regulation in Non-Obese Diabetic (NOD) mice. Auton Neurosci. 2008; 138:108–113. [PubMed: 18166503]

34. Airaksinen KE, Ikaheimo MJ, Salmela PI, Kirkinen P, Linnaluoto MK, Takkunen JT. Impaired cardiac adjustment to pregnancy in type I diabetes. Diabetes Care. 1986; 9:376–383. [PubMed: 3527613]

35. Heitritter SM, Solomon CG, Mitchell GF, Skali-Ounis N, Seely EW. Subclinical inflammation and vascular dysfunction in women with previous gestational diabetes mellitus. J Clin Endocrinol Metab. 2005; 90:3983–3988. [PubMed: 15840749]

36. Katz AM. Ernest Henry Starling, his predecessors, and the "Law of the Heart". Circulation. 2002; 106:2986–2992. [PubMed: 12460884]

37. Frustaci A, Kajstura J, Chimenti C, Jakoniuk I, Leri A, Maseri A, Nadal-Ginard B, Anversa P. Myocardial cell death in human diabetes. Circ Res. 2000; 87:1123–1132. [PubMed: 11110769]

38. Fiordaliso F, Li B, Latini R, Sonnenblick EH, Anversa P, Leri A, Kajstura J. Myocyte death in streptozotocin-induced diabetes in rats in angiotensin II- dependent. Lab Invest. 2000; 80:513–527. [PubMed: 10780668]

39. Malhotra A, Vashistha H, Yadav VS, Dube MG, Kalra SP, Abdellatif M, Meggs LG. Inhibition of p66ShcA redox activity in cardiac muscle cells attenuates hyperglycemia-induced oxidative stress and apoptosis. Am J Physiol Heart Circ Physiol. 2009; 296:H380–388. [PubMed: 19060130]

40. Debrah DO, Novak J, Matthews JE, Ramirez RJ, Shroff SG, Conrad KP. Relaxin is essential for systemic vasodilation and increased global arterial compliance during early pregnancy in conscious rats. Endocrinology. 2006; 147:5126–5131. [PubMed: 16873529]

41. Acharya G, Wilsgaard T, Berntsen GK, Maltau JM, Kiserud T. Doppler-derived umbilical artery absolute velocities and their relationship to fetoplacental volume blood flow: a longitudinal study. Ultrasound Obstet Gynecol. 2005; 25:444–453. [PubMed: 15816007]

42. Byun YJ, Kim HS, Yang JI, Kim JH, Kim HY, Chang SJ. Umbilical artery Doppler study as a predictive marker of perinatal outcome in preterm small for gestational age infants. Yonsei Med J. 2009; 50:39–44. [PubMed: 19259346]

43. Corrigan N, Treacy A, Brazil DP, McAuliffe FM. Cardiomyopathy and Diastolic Dysfunction in the Embryo and Neonate of a Type 1 Diabetic Mouse Model. Reprod Sci. 2012

44. Holmes VA, Young IS, Patterson CC, Pearson DW, Walker JD, Maresh MJ, McCance DR. Optimal glycemic control, pre-eclampsia, and gestational hypertension in women with type 1 diabetes in the diabetes and pre-eclampsia intervention trial. Diabetes Care. 2011; 34:1683–1688. [PubMed: 21636798]

45. Mathiesen ER, Ringholm L, Damm P. Pregnancy management of women with pregestational diabetes. Endocrinol Metab Clin North Am. 2011; 40:727–738. [PubMed: 22108277]

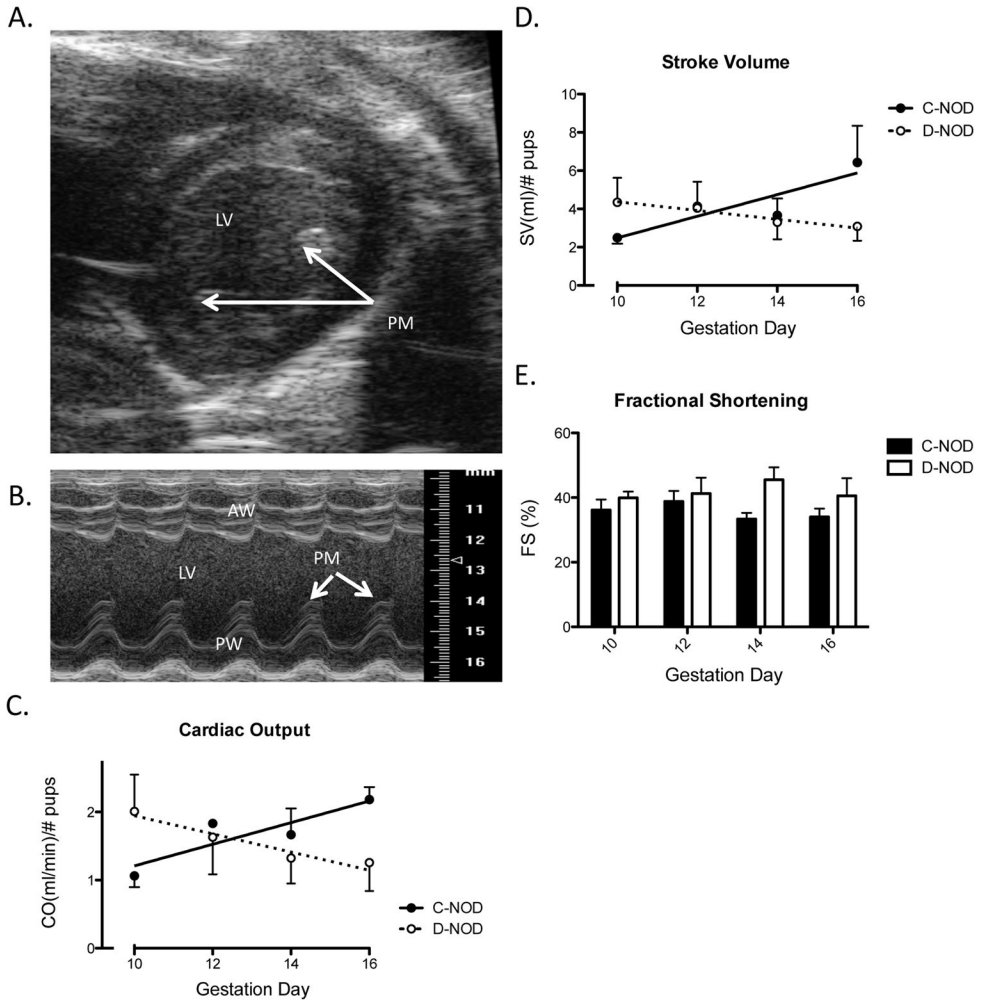

FIG. 1.

Maternal Cardiac Analyses. (A) An example of a B-Mode image of parasternal short axis view of the heart from a gd16 d-NOD. M-Mode sample volume was placed over the middle of the chamber, slightly off the papillary muscle. (B) M-Mode cine loop of parasternal short axis of the heart, also from a gd16 d-NOD. Measurements were performed excluding papillary muscle, seen as caps above the posterior wall in systole. (C) Cardiac output normalized by viable implant site number. Increasing CO is seen over gestation in c-NOD ($p=0.025$), but not d-NOD mice. Effect of gestation (analyzed via regression slopes) differed between groups ($p=0.024$). (D) Stroke volume normalized for viable implant site number. Increasing SV is seen over gestation in c-NODs ($p=0.035$). Again, no increase in SV is observed over gestation in d-NODs. Effect of gestation was different between groups ($p=0.030$). (E) Fractional shortening. FS was increased in d-NOD compared to c-NODs across the study ($p=0.0265$), however no significance was reached at any specific gd. No effect of gestation is seen on FS in either d-NOD or c-NOD dams. PM = Papillary muscle, LV = Left ventricle, AW = Anterior left ventricular wall, PW= Posterior left ventricular wall. Solid line and closed circles = c-NODs, dashed lines and open circles = d-NODs.

Significantly different slopes upon regression analysis indicated differing effects of gestation between groups, slopes by linear regression considered significantly non-zero at $p<0.05$.

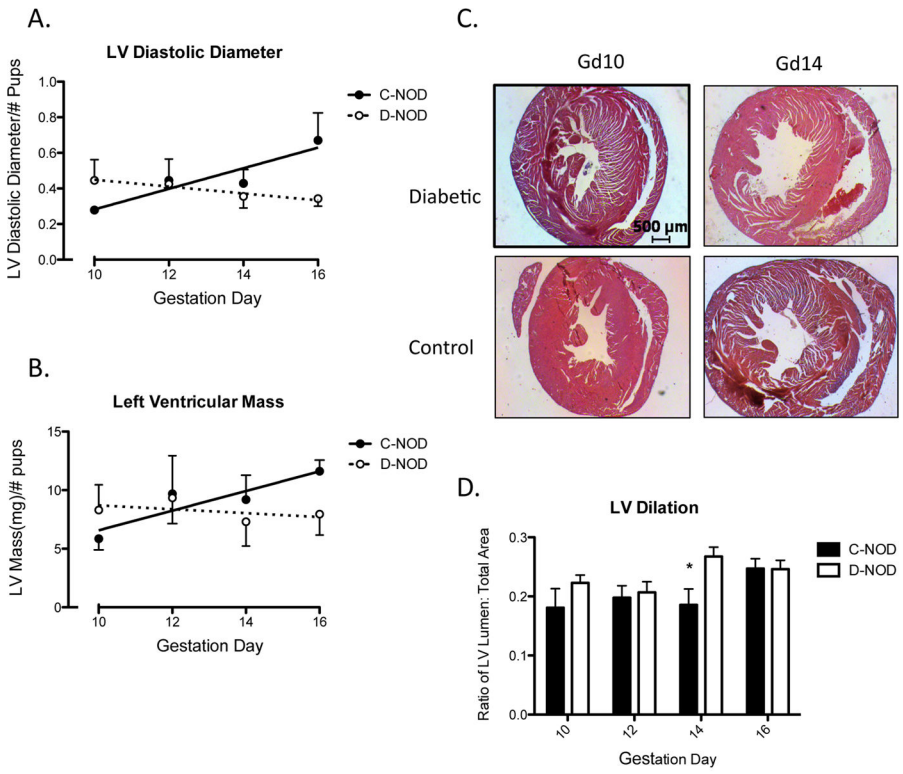

FIG. 2.

Left ventricular size and extent of dilation, calculated using ultrasonography and histological analyses. (A) Left ventricle diastolic diameter (mm) measured by ultrasound increased throughout gestation in c-NOD ($p=0.014$) but not d-NOD mice ($p=0.42$). Regression analysis showed a difference in slopes between the groups ($p=0.017$). (B) Ultrasound measurements in c-NODs showed increasing LV mass over gestation ($p=0.050$). No increase or trend was seen in d-NODs. Regression analysis showed a trend towards a difference in slopes ($p=0.15$). Values normalized to number of viable implantation sites. (C) Histological cross-sections of ventricles at the level of the papillary muscles stained with H&E, scale bar reports 500µm and refers to all panels. (D) Ratio of LV lumen area: total ventricular area was used as a measure of ventricular dilation. Overall the ratio was increased in d-NOD compared to c-NODs ($p=0.028$). Differences at specific gestation days reached significance at gd14. Ratios were measured using histological morphometry.

Solid line, closed circles and solid bars = c-NODs, dashed lines, open circles and white bars = d-NODs. * = Difference between groups. Significance between groups were determined by two-way ANOVA with $p<0.05$. Increases over gestation within groups were determined by linear regression with a non-zero slope ($p<0.05$), non-statistically significant trends over gestation defined at $p<0.15$.

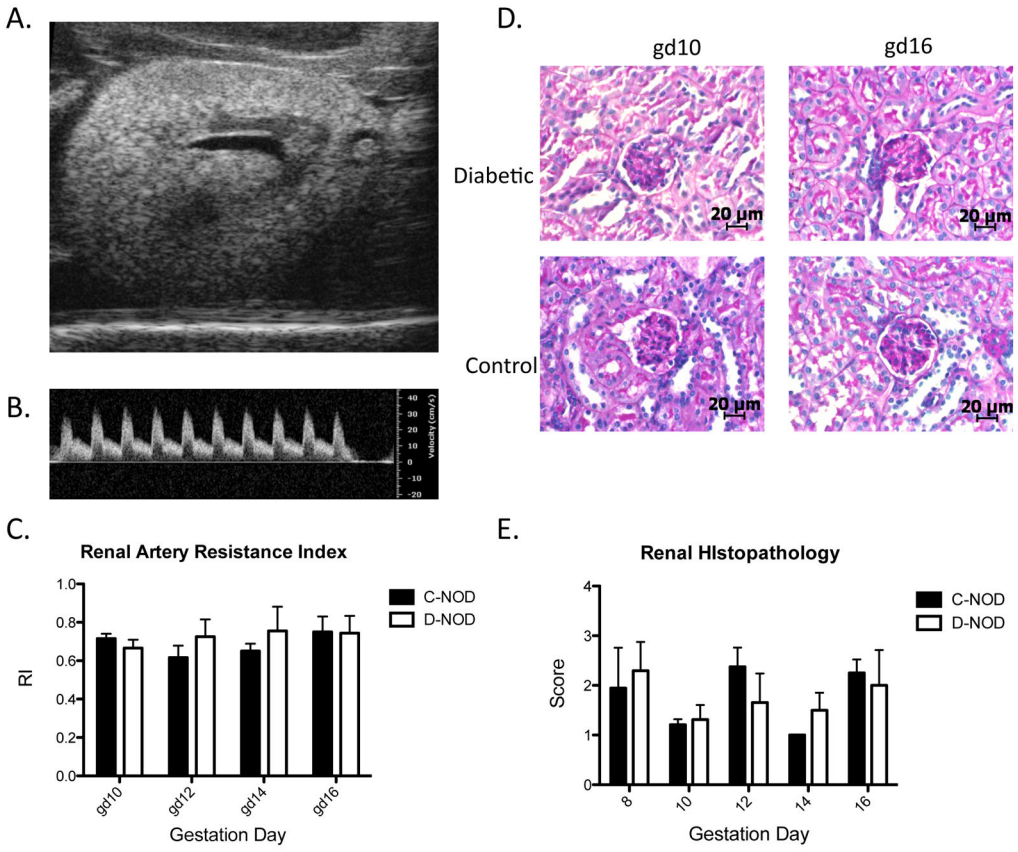

FIG. 3.

Renal physiology assessed via ultrasonography and histolopathology. (A) Example of a B-Mode image of the left kidney of a gd12 d-NOD. (B) PW Doppler of a gd10 d-NOD renal artery, measurements taken on peak systolic velocity and end diastolic velocity. (C) Renal artery RI did not differ between c-NOD and d-NODs prior to mating (data not shown) or at any gestational time-point. (D) Renal glomeruli in histological sections stained with PAS, scale bar reports 20 µm. No qualitative differences were observed between d-NOD and c-NODs from gd8 to gd16. (E) Semi-quantitative renal histopathological analysis showing no differences in renal pathology score between d-NOD and c-NODs at any gestational time-points studied. Solid bars = c-NOD, white bars = d-NOD. Difference between groups was determined by two-way ANOVA. Effect of gestation within groups was determined by linear regression.

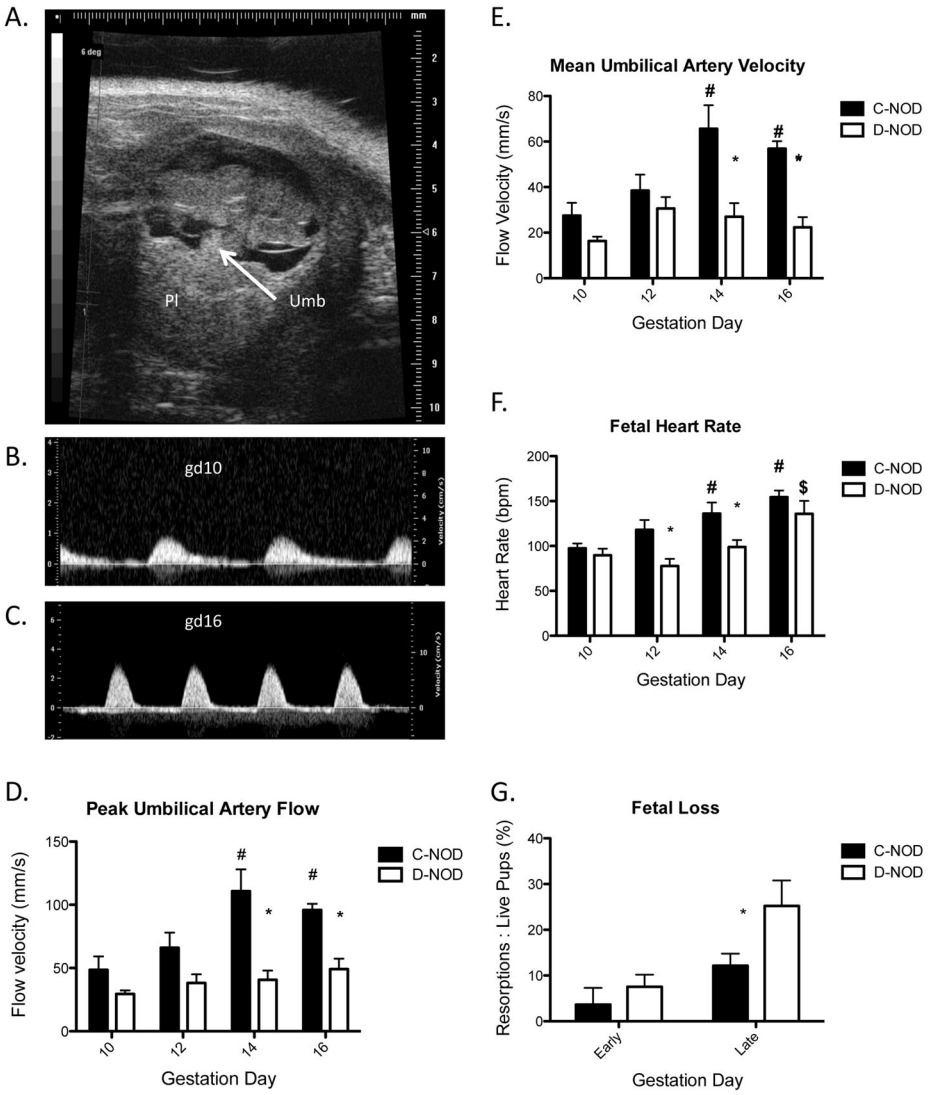

FIG. 4.

Fetal Scan. (A) Representative B-Mode image of a gd10 c-NOD fetus. (B) Representative PW Doppler image of umbilical artery in a gd10 c-NOD fetus. (C) Representative PW Doppler image of the umbilical artery in a gd16 c-NOD fetus. (D) Umbilical artery peak flow velocities, C-NODs showed an increase with increasing gestation ($p=0.0012$). Within time-points, c-NOD flow velocities are increased compared to d-NODs ($p<0.0001$), peak differences at gd14 and gd16 ($p<0.001$, $p<0.05$, respectively). A significant interaction was present between variables ($p=0.047$). (E) Umbilical artery mean flow velocities. C-NOD but not d-NOD peak flow velocities increased over gestational time-points measures ($p=<0.0001$) and differences between groups peaked at gd14 and gd16 ($p<0.001$, $p<0.01$, respectively). (F) Fetal heart rates. Similar to umbilical flow velocity, c-NOD fetal heart rates increased throughout gestation ($p<0.0001$) and are, overall, higher than fetuses of d-NOD dams ($p<0.001$). (G) Fetal loss as measured by percentage of resorptions to viable pups. Overall, fetal loss was elevated in d-NOD compared to c-NODs ($p=0.036$). Early gestation days for this study were defined as gd10 and 12, later gestation days were defined

as gd14 and 16. Differences between groups did not differ at early gestation days but reached significance at later gestation days ($p<0.05$).

Minimum n=9 per group for all ultrasound data (minimum of three fetuses per dam, 3 dams per group at each gd). Significance between groups at each gestation day determined by two-way ANOVA with Bonferroni's post-test, with $p<0.05$. Effect of gestation within each group determined by linear regression, increases and decreases over time defined by non-zero slope with $p<0.05$. Solid bars = c-NOD, white bars = d-NOD. Umb = Umbilical cord, Pl = Placenta. Single asterisks = significance between glycemic groups; hash tag = significance from gd10; dollar sign = significance from gd12.

TABLE 1

Maternal Characteristics

Gestation Day		Virgin	gd8	gd10	gd12	gd14	gd16	Overall
Body weight (g)	Control	26.9±1.4	26.8±0.6	27.7±0.7	28.7±1.8	29.8±1.5	33.4±2.0	
	Diabetic	23.5±0.2	24.5±1.4	27.1±2.5	30.4±1.2	29.2±1.4	31.1±0.9	
	p value	NS	NS	NS	NS	NS	NS	NS
Initial Blood Glucose (mmol/L)	Control		6.4±0.6	5.5±0.3	5.9±0.3	4.9±0.4	5.5±0.5	
	Diabetic		26.3±4.2	19±1.9	24.9±2.1	21.3±1.2	21.8±1.5	
	p value		0.0001	< 0.0001	< 0.0001	< 0.0001	< 0.0001	< 0.0001
Final Blood Glucose (mmol/L)	Control	6.3±0.6	8.7±0.4	8±0.4	7.8±1.1	6±0.5	6.3±0.6	
	Diabetic	28.6±0.9	30.2±1.3	30.0±1.9	27.7±2.8	31.4±1.0	31.0±2.3	
	p value	< 0.0001	< 0.0001	< 0.0001	< 0.0001	< 0.0001	< 0.0001	< 0.0001
Viable Litter Size	Control		10.7±0.9	11.3±0.3	7.7±1.3	8±1.2	5.7±0.9	
	Diabetic		11±0	8.3±1.8	8.7±1.9	8.7±0.9	6.7±2.9	
	p value		NS	NS	NS	NS	NS	NS
Maternal Heart Rate (BPM)	Control	433.2±15.8	442.9±13.5	422.2±26.4	449.5±7.3	479.4±21.8	486.9±2.3	
	Diabetic	425.3±22.3	449.8±6.7	427.1±8.9	407.0±1.6	402.5±18.0	380.3±44.3	
	p value	NS	NS	NS	NS	NS	0.006	0.005

Significant differences between groups overall and at each individual time-point were determined by two-way ANOVA with Bonferroni's post-test.